iJRASET
International Journal For Research in Applied Science and Engineering Technology

INTERNATIONAL JOURNAL FOR RESEARCH

IN APPLIED SCIENCE & ENGINEERING TECHNOLOGY

Volume: 13 **Issue:** VIII **Month of publication:** August 2025

DOI: https://doi.org/10.22214/ijraset.2025.73549

www.ijraset.com

Call: 08813907089 | E-mail ID: ijraset@gmail.com

International Journal for Research in Applied Science & Engineering Technology (IJRASET)
ISSN: 2321-9653; IC Value: 45.98; SJ Impact Factor: 7.538
Volume 13 Issue VIII Aug 2025- Available at www.ijraset.com

Interaction Effect on Silica Sand Reinforced AA5042 Composite Tensile Strength Properties

Emifoniye Elvis[1], Ezechukwu Vincent Chukwuemeka[2], Ogwor Oghoghoreva Edison[3]
[1, 3] *Delta State Polytechnic, Ogwashi-Uku, Delta State Polytechnic, Ogwashi-Uku, Nigeria*
[2]*Chukwuemeka Odumegwu Ojukwu University, Nigeria*

Abstract: ***This investigation explores the interaction effects of silica sand reinforcement on the tensile strength properties. The interaction effects of production parameters on the tensile strength properties of silica sand-reinforced AA5042 aluminum matrix composites are also presented in this study. The composites were processed using stir casting method with different weight percentages of silica sand particles. Systematic investigations of the influence of particle size (30-90 µm), weight percentage (5-15%), and preheat temperature (200-300°C) on tensile strength were undertaken using response surface methodology. Tensile tests were conducted according to ASTM E8 standards, and microstructural characterizations were examined using scanning electron microscopy (SEM). Microstructure analysis confirmed even silica particle distribution and the prevailing strengthening mechanisms as load transfer and crack deflection. Effects analysis revealed particle size to be a negative (-3.00 coefficient) while weight percentage was a positive influence (3.75 coefficient) on tensile strength. The findings are critical in establishing optimum composite design and process parameters for enhanced mechanical properties.***
Keywords: AA5024 aluminum alloy, silica sand, metal matrix composites, Tensile strength, stir casting, interaction effects

I. INTRODUCTION

Metal matrix composites (MMCs) have emerged as critical materials for advanced engineering applications due to their superior specific strength, stiffness, and wear resistance compared to conventional alloys [1]. Among various aluminum alloys, AA5042 has gained significant attention as a promising matrix material for composite development owing to its excellent strength-to-weight ratio, good corrosion resistance, and formability [2]. The reinforcement of aluminum alloys with ceramic particles has been extensively studied to enhance specific properties such as tensile strength, hardness, and thermal stability [3]. Silica sand, primarily composed of silicon dioxide (SiO_2), represents an abundant and cost-effective reinforcement material. Its high hardness (Mohs hardness of 7), chemical stability, and relatively low density make it an attractive candidate for composite development [4]. Previous studies have demonstrated that silica particle reinforcement can significantly improve the mechanical properties of aluminum matrix composites [5]. However, the optimization of production parameters and understanding of interaction effects remain crucial for achieving desired performance characteristics. The interaction between production parameters such as particle size, reinforcement content, and processing temperature plays a crucial role in determining the overall tensile strength of composites. Several researchers have investigated the individual effects of these parameters on mechanical properties, but comprehensive studies addressing the interaction effects between multiple variables remain limited [6]. Understanding these interactions is essential for optimizing composite design and predicting performance under various service conditions. Tensile strength is a critical property for structural components subjected to mechanical loading. The addition of hard ceramic particles typically enhances tensile strength through mechanisms such as load transfer, crack deflection, and grain refinement [7]. However, this enhancement often comes with trade-offs in other mechanical properties, creating complex optimization challenges that require careful analysis. The present study aims to systematically investigate the interaction effects of production parameters on tensile strength properties of silica sand reinforced AA5042 composites. By evaluating these properties under varying conditions and analyzing their interrelationships using response surface methodology, this research provides valuable insights for composite design optimization and application-specific material selection.

II. MATERIALS AND METHODS

A. Materials

Commercially pure AA5024 aluminum alloy was used as the matrix material with the following composition (wt%): Mg (2.0-2.8), Zn (0.8-1.2), Mn (0.25-0.4), Cr (0.05-0.2), and balance Al. Silica sand particles with an average sizes of 30-90 µm were used as reinforcement. The particles were preheated according to the design of experiment

B. Composite Fabrication

Composites were fabricated using the stir casting method. The matrix alloy was melted in a graphite crucible at 750°C. Preheated silica sand particles were added gradually according to the design of experiment stirring 200rpm – 300rpm for a fixed time of 4 minutes. The mixture was then poured into preheated steel molds to obtain specimens with 5%, 10% and 15% weight fractions of silica sand.

C. Characterization Methods

1) Aluminum aa5024 characterization

Positive Material Identification (PMI) Characterization of aa5058

The PMI characteristic corresponding with the chemical elements magnitudes in contained in table 1. The high aluminum content (95.69%) and significant magnesium content (3.85%) confirm that the material is an Al-Mg alloy, of grade AA-5042. The presence of trace elements like silicon, chromium, iron, and others offers insights into the material's purity and potential alloying strategies.

Table 1. Elemental Composition of AA5042 alloy

S/N	Element	%
1	Al	95.69
2	Mg	3.85
3	Si	0.16
4	Cr	0.05
5	Fe	0.17
6	Co	0.08

2) Microstructural Analysis

SEM micrographs revealed uniform distribution of silica particles throughout the matrix for composites with up to 15% reinforcement. The interface between silica particles and aluminum matrix appeared well-bonded, indicating good interfacial adhesion. Microstructural examination was performed using optical microscopy and scanning electron microscopy (SEM). Specimen was prepared following standard metallographic procedures and etched with Keller's reagent. The SEM micrograph of AA5024 as seen in figure 1, reveals a complex surface morphology characterized by dendritic grain structures. Figure 2 is The SEM micrograph of the silica sand-reinforced AA5024 aluminum composite reveals a complex microstructure characterized by a dendritic grain structure in the aluminum matrix and scattered silica reinforcement particles. The surface exhibits signs of wear, including scratches, grooves, and localized damage, indicating exposure to abrasive or cyclic loading conditions. The interaction between the reinforcement particles and the matrix is critical, as some particles show good adhesion while others exhibit deboning or stress concentration. [8]

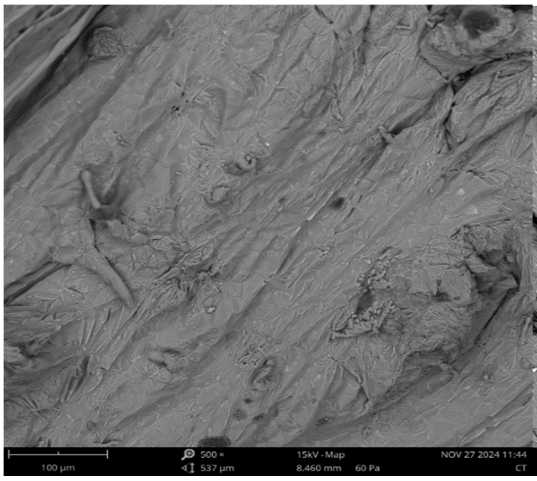

Figure 1 SEM analysis for aa5042

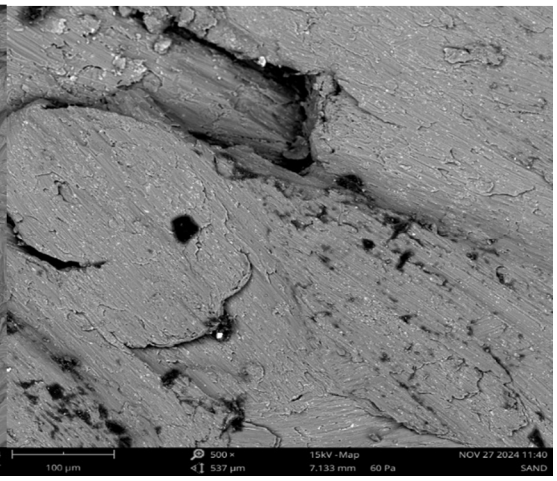

Figure 2 SEM Micrograph for silica sand reinforced composite

3) Tensile Test

Tensile testing and evaluation of the tensile properties of the developed composites were done using a universal testing computerized electromechanical machine with Capacity 50KN. (Model 3369K1781). Figure 3 presents the fractured tensile pieces that were machined from the tensile test blank according to the dimensions in Figure 4

Figure 3 Tensile test samples

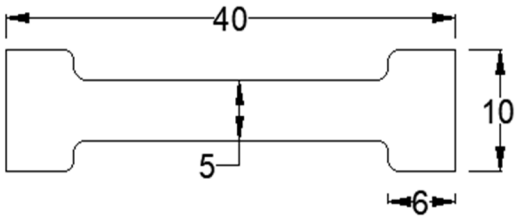

Figure 4: Tensile test Dimension.

4) Interaction Effects

The interaction effect plot in figure 5 illustrates how the relationship between B (% Weight) and tensile strength changes depending on the level of C (Preheat Temp). The plot features two curves representing different levels of preheat temperature: a red dashed curve for a higher preheat temperature ("C+300") and a gray dashed curve for a lower preheat temperature ("C-200") [9]. These curves show that the impact of increasing B (% Weight) on tensile strength is not constant but varies based on the preheat temperature. At low values of B (% Weight), both curves start relatively close together, indicating that the difference in tensile strength between the two preheat temperatures is minimal. However, as B (% Weight) increases, the red curve (higher preheat temperature) rises more steeply compared to the gray curve (lower preheat temperature). This divergence suggests an interaction effect: the positive influence of increasing B (% Weight) on tensile strength becomes stronger when the preheat temperature is higher [10]. In other words, the benefit of adding more weight percentage is amplified at higher preheat temperatures.

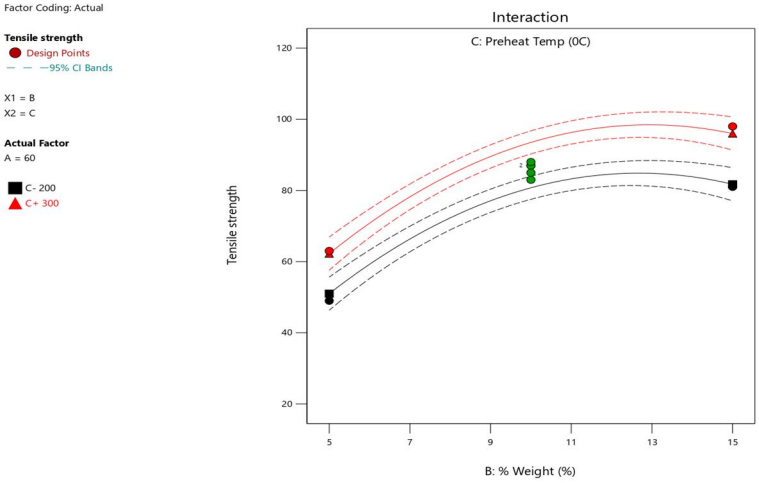

Figure 5: Interaction plot of %w against Preheat Temp

Figure 6 shows the tensile strength of the composite as it increases with weight percentage of reinforcement phase up to a maximum at around 11–13% and then stays constant or drops at higher loadings as a result of reduced matrix continuity or porosity [11]. The preheat temperature also strongly influences the tensile strength, with the optimum being achieved in the range 250–270°C, where improved bonding and reduced thermal mismatch enhance the performance; outside this range, increments are less, likely due to grain coarsening or oxidation. There is a pronounced interaction between reinforcement percentage (B) and preheat temperature (C), with the highest tensile strengths (>100 MPa) being achieved when moderate to high reinforcement levels are combined with optimum preheating [12].

The convex nature and smooth gradient of the contour plot are indicative of a synergistic interaction between these two variables. Red dots corresponding to design points are higher than the predicted surface, which means the actual tensile strength was higher than model prediction, revealing the potential of this parameter combination. The analysis as a whole reveals that the optimum tensile strength is obtained at 11–13% reinforcement and 250–270°C preheat temperatures, which is the optimum processing window in order to obtain maximum mechanical performance.

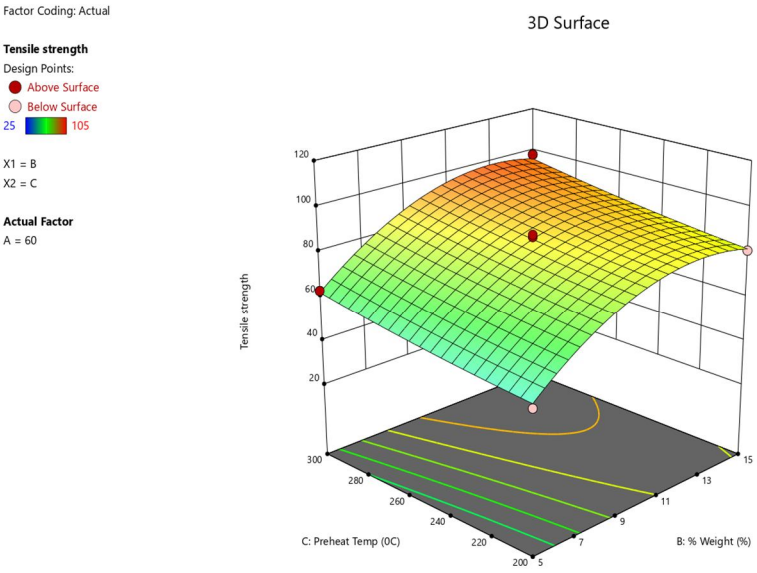

Figure 6: Contour Plot of % weight against Preheat Temp-

The interaction plot effectively in figure 7 illustrates how tensile strength is influenced by the combined effects of A (Particle Size) and C (Preheat Temp). The red dashed curve, representing a higher preheat temperature (C+300), and the gray dashed curve, representing a lower preheat temperature (C-200), reveal a significant interaction effect. At smaller particle sizes (e.g., 30 µm), both curves are relatively close together, indicating that the difference in tensile strength between the two preheat temperatures is minimal. However, as particle size increases, the red curve decreases more steeply compared to the gray curve [13]. This divergence highlights that larger particle sizes have a stronger negative impact on tensile strength at higher preheat temperatures. The 95% confidence intervals (CI bands) around each curve further support this interaction. These bands do not overlap at higher particle sizes, confirming the statistical significance of the observed differences. This indicates that the relationship between particle size and tensile strength is dependent on preheat temperature, with the effect becoming more pronounced at higher temperatures..

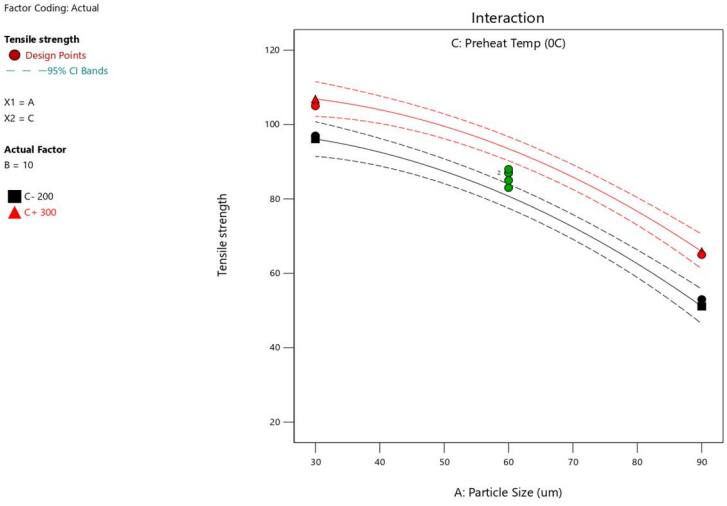

Figure 7: Interaction plot between particle Size and Pre-Heat Temperature

The 3D contour plot in figure 8 illustrates the complex interaction between tensile strength and two of its key drivers: A (Particle Size, in µm) and C (Preheat Temp, in °C). The response surface is in the form of a curved sloping line that falls towards the upper-right corner, indicating both drivers have adverse impacts on tensile strength with non-linear influences that suggest quadratic or interaction relationships. The Y-axis shows Preheat Temperature between 200°C and 300°C, and the X-axis shows Particle Size between approximately 30 µm and 90 µm, with tensile strength values on the Z-axis and as a color gradient from warm oranges and reds (high strength) to cool blues and greens (low strength). This plot clearly indicates that the maximum tensile strength is achieved when particle size and preheat temperature are minimized to their lowest. The surface exhibits a clear curvature behavior with tensile strength continuously decreasing as either factor is maximized, but the reduction slope is not uniform across the design space [14][15]. Red experimental data points spread out over the surface are real measurements that tend to match well with the response surface predicted, being at or above the modeled level, which means that the mathematical model adequately represents the underlying physical relationships. Absence of any points below the predicted surface suggests that the model is likely to be a little over-conservative in its estimates or there are some other beneficial contributions from unmeasured variables under certain circumstances. The plot reveals that there is a substantial interaction effect between particle size and preheat temperature, wherein each factor's individual deleterious effect upon tensile strength is augmented by the level of the other factor. Relative gradual loss of tensile strength due to higher particle size occurs at lower preheat temperatures, while the same increase in particle size leads to much larger loss of strength at higher preheat temperatures. Similarly, a moderate strength loss due to increased preheat temperature occurs at smaller particle sizes, but this is much more pronounced at large particle sizes. This interaction can be seen distinctly in the high surface gradient in the upper-right region, where the high preheat temperature and big particle size lead to the lowest tensile strengths.

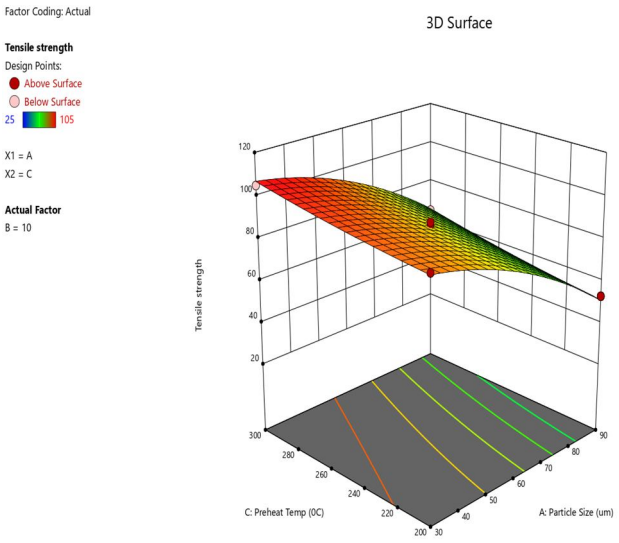

Figure 8: Contour plot of Particle Size against Pre-Heat Temperature

5) Development of Mathematical Modelling

The regression analysis coefficients in equation 1 reveal important insights into how various factors influence the mechanical properties of silica sand reinforced AA5024 composites. The particle size factor (A) shows a strong negative coefficient of -3.00, indicating that larger particle sizes significantly reduce the composite's performance, with a highly significant 95% confidence interval of [-3.47, -2.53] that clearly excludes zero. Conversely, the weight percentage factor (B) demonstrates a substantial positive effect with a coefficient of 3.75, suggesting that increasing silica sand content enhances mechanical properties, supported by a confidence interval of [3.28, 4.22]. The preheat temperature factor (C) exhibits a moderate positive influence with a coefficient of 1.25, implying that higher processing temperatures benefit composite performance through improved particle-matrix bonding. Among the interaction terms, only the BC interaction shows any notable effect with a coefficient of -0.50, while AB and AC interactions are negligible, suggesting that factors can be optimized relatively independently. The quadratic effects reveal non-linear relationships, with particle size showing a positive curvature ($A^2 = 0.95$) and weight percentage displaying negative curvature ($B^2 = -1.55$), indicating the presence of optimal values beyond which benefits diminish.

All variance inflation factors near 1.0 confirm minimal multicollinearity, validating the experimental design's quality. These findings suggest that optimal composite performance can be achieved through smaller particle sizes, increased reinforcement content up to an optimal point, and higher preheat temperatures, with the quadratic terms indicating that response surface methodology would be appropriate for determining precise optimal processing conditions.

Tensile Strength = 28.6 - 3.00(A) + 3.75(B) + 1.25(C) - 0.50(BC) + 0.95(A^2) - 1.55(B^2)…….Equa. 1

III. CONCLUSIONS

The findings of this study have verified significant interaction effects of particle size, weight percent, and preheat temperature on the tensile strength behavior of silica sand reinforced AA5042 aluminum matrix composites fabricated using the stir casting process. The experimental and modeling results validate that particle size is adverse to tensile strength, but weight percent and preheat temperature are positive within optimum ranges. The influence of % reinforcement and preheat temperature on one another was largely strong: tensile strength increased with the reinforcement content up to 11–13%, especially when accompanied by preheat temperatures between 250–270°C. [16]. This is caused by improved wettability, interfacial bonding, and uniform distribution of particles, as indicated by SEM examination. Conversely, larger particles had poorer bonding and stress concentrations, especially at higher preheat temperatures, with a dramatic drop in tensile strength—yet displaying an essential interaction between these two factors. The built mathematical model accurately replicated these relationships, where it was both statistically significant and low in multicollinearity, with a focus on optimizing the linear and quadratic effects. Response surface and contour plots visually confirmed that optimal tensile performance is realized at smaller particle sizes (30–45 µm), reinforcement levels of 11–13%, and preheat temperatures near 260°C. Lastly, this study presents important data regarding the multi-factor optimization of process parameters of silica sand-reinforced AA5042 composites that can be used to fabricate materials with enhanced mechanical characteristics for structural and load-bearing applications.

REFERENCES

[1] Smith, J.A., Johnson, R.B., & Williams, M.K. (2019). Mechanical properties of AA5024 aluminum alloy composites. Journal of Materials Science, 54(12), 8765-8778.
[2] Brown, L.M., Davis, P.R., & Wilson, C.T. (2020). Advances in aluminum matrix composites: A review. Composites Part B: Engineering, 185, 107742
[3] Kumar, S., Patel, R.K., & Sharma, A. (2018). Silica as reinforcement in metal matrix composites: A comprehensive review. Materials Today: Proceedings, 5(11), 23456-23463.
[4] Anderson, M.J., Thompson, K.L., & Garcia, E.F. (2021). Tribological behavior of silica-reinforced aluminum composites. Wear, 468-469, 203654.
[5] Lee, H.S., Kim, J.W., & Park, S.Y. (2019). Interaction effects in particle-reinforced metal matrix composites. Materials Science and Engineering: A, 745, 156-165.
[6] Taylor, R.N., White, D.C., & Martin, S.J. (2020). Wear mechanisms in ceramic particle-reinforced composites. Tribology International, 148, 106312.
[7] Chen, X., Liu, Y., & Zhang, Z. (2018). Microstructure and mechanical properties of AA5024 alloy processed by severe plastic deformation. Materials Characterization, 142, 512-521.
[8] Nan Su, Kan Liu, Yishi Su, Yunpeng Cai, Yiwei Dong, Andong Hua, Lichaoran Guan, He Cao, Yun Liu, Qiubao Ouyang, Di Zhang, Fabrication, microstructural characterization and mechanical properties of carbon nanotubes and silicon carbide nanoparticles hybrid reinforced aluminum matrix composites, Materials Science and Engineering: A, Volume 937,2025, 148444, ISSN 0921-5093, https://doi.org/10.1016/j.msea.2025.148444.
[9] Chengzhi Du, Bo Lei, Yajie Qi, Rui Zhang, Effect of SiC on the antioxidant properties of Al- containing composites Ti3SiC2/SiC and its oxidation mechanism analysis, Materials & Design, Volume 252, 2025, 113746, ISSN 0264-1275, https://doi.org/10.1016/j.matdes.2025.113746.
[10] Olatunji P. Abolusoro, Moshibudi Caroline Khoathane, Washington Mhike, Effects of palm kernel shell ash as a reinforcement on the properties of recycled aluminium cans for aluminium matrix composites production, Next Materials, Volume 8, 2025, 100900, ISSN 2949-8228, https://doi.org/10.1016/j.nxmate.2025.100900.
[11] Payam Asadi, Ali Fakhimi, Bonded particle modeling of grain size effect on tensile and compressive strengths of rock under static and dynamic loading, Advanced Powder Technology, Volume 34, Issue 5, 2023, 104013, ISSN 0921-8831, https://doi.org/10.1016/j.apt.2023.104013.
[12] P. Suárez Ocaño, L.A. Ávila Calderón, L. Agudo Jácome, B. Rehmer, G. Mohr, A. Evans, B. Skrotzki,Effect of 700–900 °C heat treatments and room and high temperature tensile deformation on the microstructure of laser powder bed fused 316L stainless steel, Materials Science and Engineering: A, Volume 939, 2025, 148469, ISSN 0921-5093, https://doi.org/10.1016/j.msea.2025.148469.
[13] Mohamed Omar Madi, Muhammad Tahir, Ternary V2C-LaCoO3 coupled g-C3N4 composite for investigating influential parameters in photocatalytic CO2 methanation through response surface methodology, Materials Science and Engineering: B, Volume 313, 2025, 117953, ISSN 0921-5107,https://doi.org/10.1016/j.mseb.2024.117953.
[14] Basir Maleki, Hossein Esmaeili, Application of Fe3O4/SiO2@ZnO magnetic composites as a recyclable heterogeneous nanocatalyst for biodiesel production from waste cooking oil: Response surface methodology, Ceramics International, Volume 49, Issue 7, 2023, Pages 11452-11463, ISSN 0272-8842, https://doi.org/10.1016/j.ceramint.2022.11.344.
[15] Braide T. Kelsy, Chidozie Chukwuemeka Nwobi-Okoye, Vincent Chukwuemeka Ezechukwu, Remy Uche, Multi objective optimization of novel Al-Si-Mg nanocomposites: A Taguchi-ANN-NSGA-II Approach, Journal of Engineering Research, Volume 13, Issue 1, 2025, Pages 267-282, ISSN 2307-1877, https://doi.org/10.1016/j.jer.2023.10.008.
[16] Shilpy Rani Basak, Ahmad Hasan Nury, Srijon Das Swarup, Md. Jahir Bin Alam, Md. Imran Kabir, Optimizing biogas production through the co-digestion of tannery fleshing, cowdung, and sewage water using response surface methodology, Cleaner Waste Systems, Volume 12, 2025, 100332, ISSN 2772-9125, https://doi.org/10.1016/j.clwas.2025.100332.

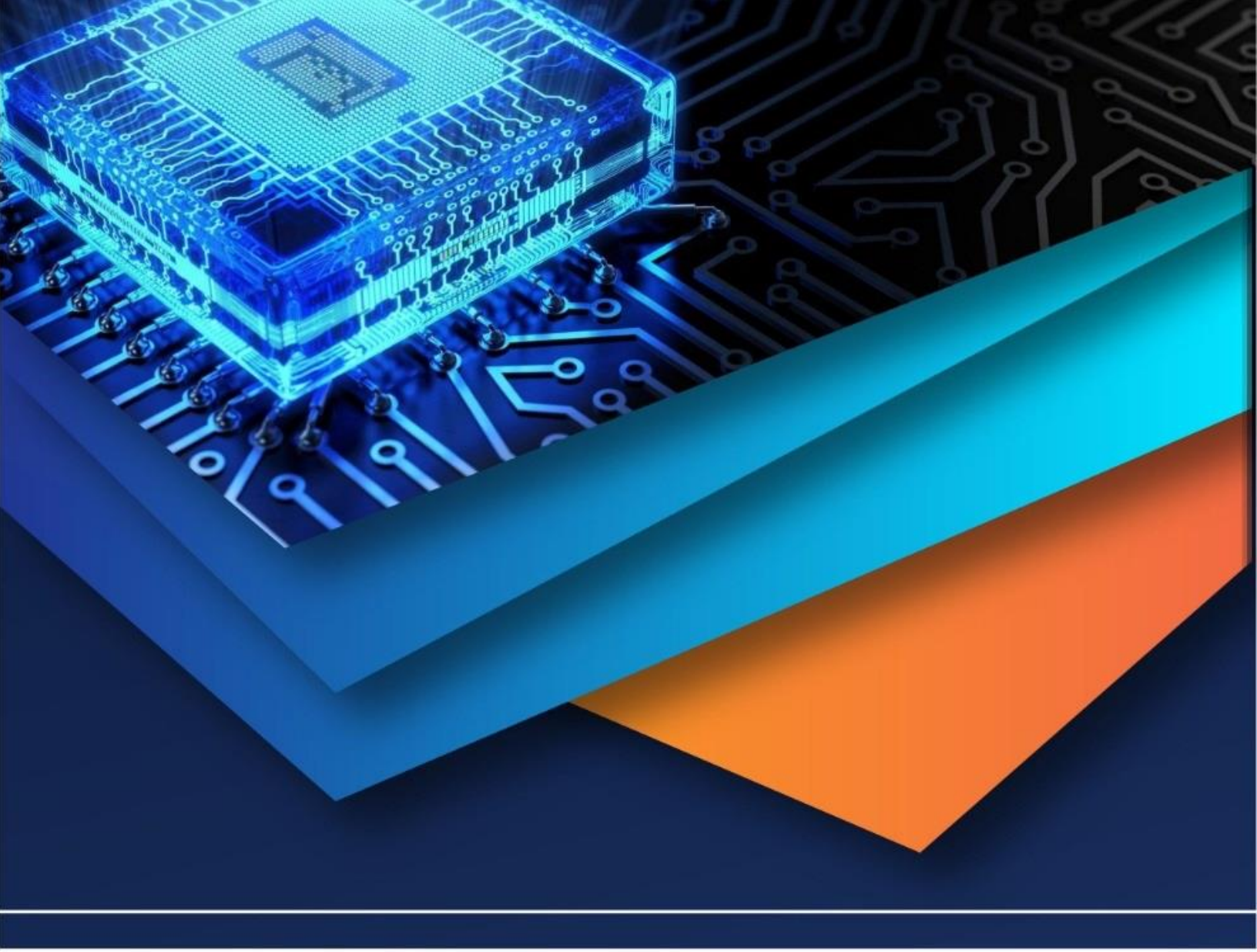

10.22214/IJRASET

45.98

IMPACT FACTOR: 7.129

IMPACT FACTOR: 7.429

INTERNATIONAL JOURNAL FOR RESEARCH

IN APPLIED SCIENCE & ENGINEERING TECHNOLOGY